



Effect of different pore membrane on ultrafiltration treatment of wastewater contained heavy metals complexed by palygorskite

Jun Ren^{a,b,c,*}, Zhongxing Li^a, Yilei Zhou^a, Lei Huang^a, Ben Ma^a, Jiaxuan Pan^a,
Ling Tao^{a,b,c}

^aKey laboratory of Yellow River Water Environment in Gansu Province, Lanzhou Jiaotong University, Lanzhou 730070, emails: renjun@mail.lzjtu.cn (J. Ren), 462507687@qq.com (Z. Li), 782352742@qq.com (Y. Zhou), 747197086@qq.com (L. Huang), 845530816@qq.com (B. Ma), 1912188772@qq.com (J. Pan), taoling@mail.lzjtu.cn (L. Tao)

^bSchool of Environmental and Municipal Engineering, Lanzhou Jiaotong University, Lanzhou 730070, P.R. China

^cGansu Hanxing Environmental Protection Co., Ltd., Lanzhou 730070, China

Received 25 April 2022; Accepted 5 October 2022

ABSTRACT

The treating effects of four hollow fiber membranes on heavy metals complexed by palygorskite in wastewater by complexation–ultrafiltration were investigated. The membranes contained three asymmetric polysulfone membranes and a polyethersulfone membrane with nominal molecular weight cut-off (MWCO) between 6,000 and 100,000 Da. The results through the comprehensive analysis of the rejection rate and the flux of normalized membranes showed that 6,000; 10,000 and 6,000 Da ultrafiltration membranes were suitable for the ultrafiltration of Cu²⁺, Zn²⁺, Cd²⁺, respectively. The pseudo-first-order reaction rate equation can better represent the reaction behavior of the complexes of favorite-ultraviolet at four membrane pore sizes. Four kinds of ultrafiltration membranes with molecular weight cut-offs of 6, 10, 50, and 100 kDa were fouled with wastewater containing Cu²⁺, Zn²⁺, Cd²⁺ complexed by palygorskite in complexation–ultrafiltration process at a transmembrane pressure of 1 bar and 20°C. The influence of molecular weight cut-off was investigated. The permeation flux decreased with time. Permeate flux declined with time gradually and finally stabilized after about 140 min of operation for all the membranes tested. 50,000 Da membrane showed the highest flux decline. The concentration of heavy metals and types of materials affect the distribution of resistance. The highest proportion of resistance for 6,000 and 10,000 Da membranes is the resistance of the membrane. For 50,000 and 100,000 Da membranes, the highest proportion of its resistance is the filter cake layer resistance. The results provide a kind of inorganic clay complexing agent in large reserves for the complexation–ultrafiltration of heavy metal wastewater.

Keywords: Palygorskite; Ultrafiltration; Heavy metals; Complexation; Membrane fouling

1. Introduction

Polymer enhanced ultrafiltration (PEUF) was an effective method to remove metal ions from sewage by complexation with water-soluble polymers and ultrafiltration, where the formation of the metal ion-polymer compound

was a vital step [1,2]. It meant that only uncombined metal ions could pass through the membrane [3]. The generation of metal ion-polymer compounds were mainly contributed to electrostatic attraction and/or electron coordination which interacted between electron donors and acceptors [4,5]. In addition to treating industrial effluents from battery manufacturing, mining operations, and chlor-alkali

* Corresponding author.

processes, PEUF had also been proven to be useful in treating effluents from nuclear facilities, which could be applied to separate and recover toxic radioactive compounds such as cesium, strontium, technetium, and actinides [6,7].

Currently, the application of PEUF in removing metal ions from sewage has great potential to be explored further by researchers. Ultrafiltration (UF) membranes have been widely used in the wastewater treatment field such as heavy metal wastewaters [8–10]. However, membrane fouling which caused by a large amount of suspended matter made of metal ion-polymer compounds is one of the major issues in the UF process [11,12], which can be classified as hydraulically reversible and irreversible [13,14]. The most important consequence of membrane fouling is the gradual permeate flux decline during filtration time [15–17]. The causes of membrane pollution can be divided into internal and external causes. The internal cause refers to the interaction between pollutants and membrane surface or membrane characteristics (hydrophilicity, pore size and porosity), while the external cause refers to the change of cross-flow velocity, cross-membrane pressure, feed concentration and temperature during the UF operation.

In the past, organic and inorganic particles had been investigated to assess their abilities to binding heavy metal ions [18]. Standard polymeric complexing agents such as low molecular weight polyethyleneimine, polyacrylic acid, and alginate were known for their significant binding capacity, while relatively new dendritic polymers provided new opportunities to develop high-capacity nanoscale chelating agents for environmental applications [19,20]. Many living biomaterials (e.g., algae, fungus, and bacteria) were also found to adsorb heavy metal ions [21,22]. Palygorskite was known for its outstanding ion-exchange property in inorganic materials [23]. It was successfully made into nanoscale crystals to increase its potential effectiveness in chemical, biomedical, and environmental applications [24,25].

Nanoparticles complexed with metal ions are required to have high affinity for target metal, low affinity for non-target metal, high possibility of regeneration, good chemical and mechanical stability, low toxicity and low cost to improve metal removal efficiency. The critical step is the nanoparticle separation, which could be achieved through low-pressure membrane processes in a manner resembling polymer enhanced ultrafiltration (PEUF) [26,27]. Membrane characteristics like molecular weight cut-off (MWCO), physical-chemical properties (e.g., pore size, charge, material type, and hydrophobicity), fouling resistance, and energy consumption plays an important role in nanoparticle-enhanced ultrafiltration (NEUF) [28,29].

Complexation-ultrafiltration production often accompanies complicated physical and chemical reactions, where physical reactions contain rejection which means contaminants with a bigger size than the pore of the membrane can be rejected [30] and chemical reactions like adsorption with some organic matters [31]. There are two typical blocking laws that cause membrane fouling [32]. Firstly, larger particles accumulate on the membrane surface and smaller fill inside the pores; secondly, filter cake formation with more and more particle precipitation on the membrane will create high resistance and reduce membrane flux [33].

Today, UF, as a fast and efficient technology, has significant applications in drinking water production and contaminated water treatment. As membrane fouling remains a key issue limiting its wider use, fouling reduction has been the focus of its practical application in recent years [34,35]. Membrane fouling is inevitable, although pretreatment of feed, membrane material/surface modification, and control of operating parameters can reduce membrane fouling to some extent [36,37]. The researchers work hard to find a moderate pretreatment method that would integrate higher pollutant removal rates, lower permeability loss rates and lower overall process costs [38].

Current research is focused on elucidating the ability of nanoscale materials to bind heavy metal ions and then remove them from water by ultrafiltration. Kinetics, binding capacity, and regeneration of synthesized palygorskite dendrimers nanoparticles had been tested under various experimental conditions. The separation of nanoparticle metal complexes had been investigated by using ultrafiltration membranes with molecular weight cut-off ranging from 6 to 100 kDa [39,40]. This work aims to evaluate membrane fouling after ultrafiltration treatment of wastewater containing heavy metals complexed by palygorskite under different molecular weights cut off of 6, 10, 50, and 100 kDa. The influence of membrane fouling was investigated, which can guide optimizing running parameters and membrane cleaning. The study revealed the basic physical-chemical mechanisms of PEUF and its potential for practical application.

2. Material and methods

2.1. Materials

The palygorskite was provided by Gansu Hanxin Environmental Protection Co., Ltd., and collected from Banqiao Town, Linze County of Gansu Province, China. It was broken, crushed and ground, and then sieved at 200 mesh sieves. The main mineral compositions were palygorskite 29.7% (2θ of 8.49°, 22.9°, 26.7°, 30.97°, and 43.44°), quartz 21.8% (2θ of 3.34°), sepiolite 4.9% (2θ of 12.10°), feldspar 14.6% (2θ of 12.37°), dolomite 6.3% (2θ of 2.85°), chlorite 4.8% (2θ of 14.15°), gypsum 5.1% (2θ of 6.04°), montmorillonite 5.3% (2θ of 17.60°), calcite 3.2% (2θ of 3.02°), mica 4.2% (2θ of 9.35°). The main composition was SiO₂ 63.47%, Al₂O₃ 18.01%, MgO 4.20%, Fe₂O₃ 5.16% and K₂O 3.64% (Fig. 1).

Three kinds of 30 L simulated heavy metal wastewater were prepared by adding CdCl₂, CuCl₂ and ZnCl₂, and the concentration of Cd²⁺, Cu²⁺, Zn²⁺ was 10, 40 and 30 mg/L, respectively.

2.2. Apparatus

In this study, a laboratory bench-scale system of cross-flow filters was employed (Fig. 2). The functional ultrafiltration process consisted of a feed tank, retentate and permeate, which were connected with tubing and back pressure valves, a peristaltic pump, manual pressure control clips and a flow meter with a digital panel meter/display, a stirrer for mixing and a power supply. The feed tank was a 55 L Plexiglass tank containing palygorskite colloid solution or the cleaning solution. The temperature

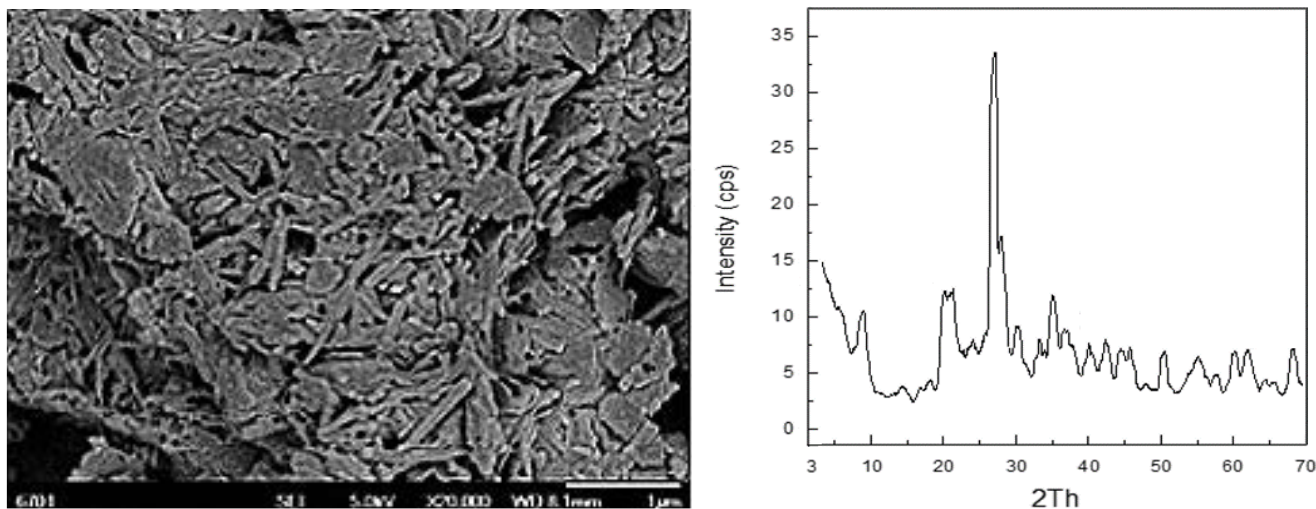


Fig. 1. Scanning electron microscopy and X-ray diffraction pattern of palygorskite.

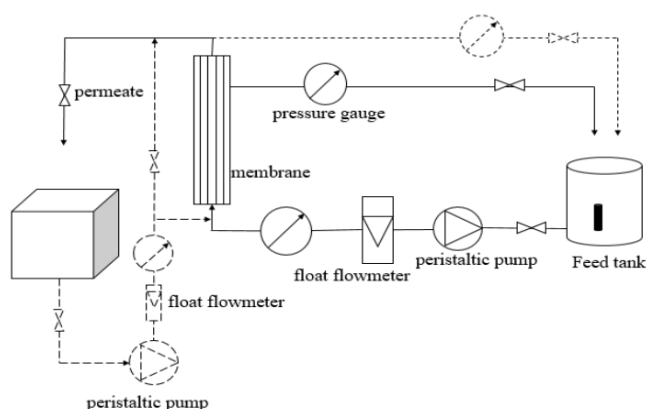


Fig. 2. The device used for ultrafiltration treatment of wastewater contained heavy metals complexed by palygorskite.

was kept constant during the experiments by the temperature regulating system. Crossflow velocity was controlled with a variable speed peristaltic pump. The maximum operating pressure was 1 bar. Pressure drop across the membrane module was measured with two manometers. A scale (0.001 g accuracy) was used to gravimetrically determine the permeate flux. The residue and permeate were recirculated back to the feed tank to keep the concentration of the feed solution constant in addition to the rinsing step.

2.3. Complexation–ultrafiltration procedure

The amount of complexing agent was 5 g/L of palygorskite at the pH of 7. All experiments were conducted at 0.1 Mpa and 25 L/h of flow rate at 20°C. pH, temperature, feed flow rate and differential pressure were monitored to be constant and observed continuously during the UF process. The complexing agent was added into 30 L 10 mg/L Cd²⁺ wastewater, 30 L 40 mg/L Cu²⁺ wastewater, and 30 L 30 mg/L Zn²⁺ wastewater. The three mixtures were kept stirring and circulating continuously through the peristaltic

pump and then passed through the 6,000; 10,000; 50,000 and 100,000 Da hollow fiber membrane respectively for 140 min all over the experiments. The four hollow fiber membranes included three different molecular weight cut-offs of polysulfone (PS) membranes (named PS6, PS10, and PS50) and polyvinylidene fluoride membrane (100,000 Da, named PVDF). The evaporation due to sampling from permeate and/or retentate may cause deviations although the feed concentration was adjusted. Thus, feed concentrations were regularly measured.

2.4. Membrane fouling experiments

Fouling tests were carried out with palygorskite colloid solution and heavy metal wastewater at a transmembrane pressure of 1 bar. The temperature of the fouling solution was set to 20°C. The duration of the fouling tests was 2.5 h. During the experiments, the permeate flux and the hydraulic resistance were monitored to check the fouling process and to ensure that reproducible values of flux and resistance were obtained in all runs.

2.5. Resistance measurement

At the end of the tests, the hydraulic resistance after the fouling step (R_f) was evaluated by means of Darcy's law.

$$J = \frac{\Delta P}{uR_t} = \frac{\Delta P}{u(R_m + R_c + R_p + R_{cp})} \quad (1)$$

where J is the permeate flux, ΔP is the transmembrane pressure, u is the feed solution viscosity and R_t is the total hydraulic resistance, R_m is the resistance of the membrane itself, Resistance of the membrane itself, R_c is the filter cake layer resistance, R_p is the blockage resistance of membrane holes, R_{cp} is the concentration polarization resistance.

Normalized membrane-specific flux is defined as the ratio of the flux of the fouled membranes (J_s) to that of the virgin membrane (J_0).

$$r = \frac{J_s}{J_0} \quad (2)$$

2.6. Statistical analysis

Membrane flux is the seepage volume of unit membrane area per unit time under a certain temperature and pressure. Membrane flux is a parameter that represents the permeability of ultrafiltration membrane and is related to the factors such as pore size, internal structure, and viscosity of slurry [41,42]. The membrane flux was measured by measuring the quality of osmotic fluid per unit of time. The quality of osmotic fluid was measured by electronic balance, and the sampling time was determined by a stopwatch. The calculation formula was as follows:

$$J_v = \frac{V}{s \times t} \quad (3)$$

where J_v is ultrafiltration membrane permeation flux, L/m²·h; V is the volume of permeation fluid, L; S is ultrafiltration membrane area, m²; and t is running time, h.

The rejection rate R , which is measured the membrane's separating capabilities is defined as:

$$R(\%) = \left(1 - \frac{c_p}{c_0} \times 100 \right) \quad (4)$$

where c_0 is the concentration of solute upstream of the membrane and c_p is the concentration of solute downstream from the membrane.

The membrane permeates flux (defined as the ratio of the pure water flux of the cleaned membranes (J_c) to that of the virgin membrane (J_0)).

$$r = \frac{J_c}{J_0} \quad (5)$$

Statistical analysis was performed based on STATISTICA. The data were analyzed through one-way analysis of variance (ANOVA) to determine the effect of membrane molecular weight cut-off and rejection coefficients, and Duncan's multiple comparison tests were performed to determine the statistical significance of the differences among means of different membrane molecular weight cut-off and permeate flux [6,43].

3. Results and analysis

3.1. Rejection coefficients

The rejection coefficient of Cu²⁺ increased strongly with the decrease of the molecular weight cut-off of the ultrafiltration membrane, and it changed little after about 120 min. The rejection coefficient increased significantly in 20 min. The rejection coefficients of the four molecular weight cut-off membranes at 120 min were increased by 11.13%, 13.82%, 16.30% and 18.64%, respectively, compared with those at 20 min. The retention coefficients were stable at 99.05%, 98.85%, 97.60% and 96.54%, respectively (Fig. 3).

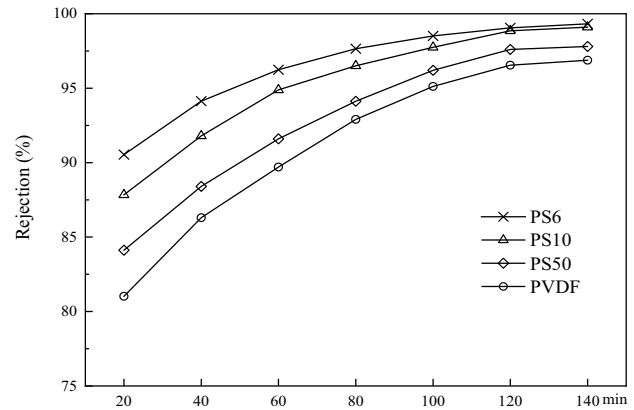


Fig. 3. The rejection coefficients of ultrafiltration treatment by four pore membranes for wastewater contained Cu²⁺ complexed by palygorskite.

The rejection coefficient of Zn²⁺ decreased strongly with the increase of the molecular weight cut-off of the ultrafiltration membrane, and it steadied after about 100 min. The rejection coefficient increased significantly in 20 min. The rejection coefficients of the four molecular weight removing ultrafiltration membranes were 92.34%, 89.20%, 86.60% and 84.13%, respectively. The rejection coefficients of the four molecular weight cut-off membranes increased by 6.41%, 8.83%, 10.96% and 12.52%, respectively, at 100 min and then stable at 98.75%, 98.03%, 97.56% and 97.05%, respectively (Fig. 4).

The rejection coefficient of Cd²⁺ decreased strongly with the increase of the molecular weight cut-offs of the membrane. The rejection of Cd²⁺ tended to be stable with different molecular weight cut-off of membrane. The removal of Cd²⁺ by the combination of the complex-ultrafiltration by palygorskite was the most intense in 20 min. The rejection coefficients of the four molecular weight cut-off membranes at 120 min were increased by 10.25%, 11.83%, 11.03%, and 8.58%, respectively, compared with those at 20 min. The rejections of Cd²⁺ were stable at 99.12%, 98.39%, 96.43%, and 93.45%, respectively (Fig. 5).

Variance analysis and multiple comparisons of the heavy metal concentrations of Cu²⁺, Zn²⁺ and Cd²⁺ in four different membranes molecular weight cut-off permeates were performed at the operating time of 120, 100 and 120 min, respectively (Fig. 6). One-way analysis of variance (ANOVA) and multiple comparisons showed that the concentrations of Cu²⁺, Zn²⁺, Cd²⁺ were significantly different in the four pore membranes ($F_{3,8} = 25.48, p < 0.001$ for Cu²⁺; $F_{3,8} = 38.65, p < 0.001$ for Zn²⁺; $F_{3,8} = 18.36, p < 0.001$ for Cd²⁺) when the operating time was 120, 100, and 120 min.

There was no significant difference in the concentration of Cu²⁺ in the permeation between PS6 and PS10 at 120 min. The amount of concentration of Cu²⁺ showed the following tendency: PVDF > PS50 > PS10 > PS6. The Cu²⁺ concentration in ultrafiltration membrane permeation liquids with molecular weight cut-offs of PS6 and PS10 was 0.38 and 0.46 mg/L, respectively, which reached the first-grade emission standard of GB 8978-1996 (<0.5 mg/L). PS6 and PS10 were selected as the post-study factors that affect the

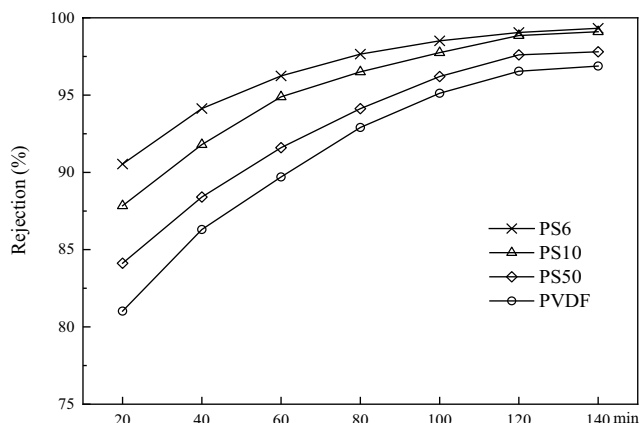


Fig. 4. The rejection coefficients of ultrafiltration treatment by four pore membranes for wastewater contained Zn^{2+} complexed by palygorskite.

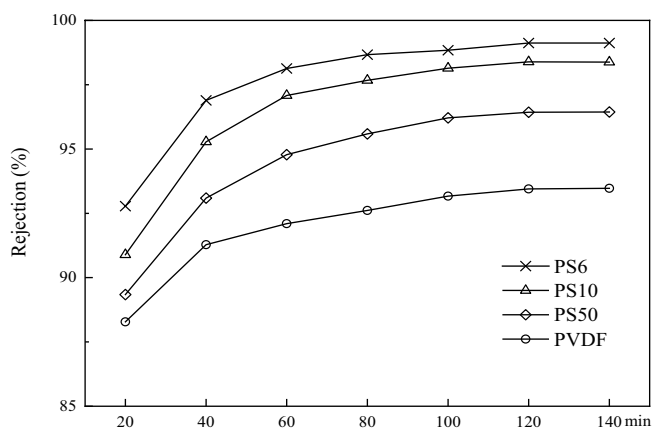


Fig. 5. The rejection coefficients of ultrafiltration treatment by four pore membranes for wastewater contained Cd^{2+} complexed by palygorskite.

preselected membrane. There was no significant difference in the concentration of Zn^{2+} in the permeation between PS6 and PS10 at 100 min. The amount of concentration of Zn^{2+} showed the following tendency: PVDF > PS50 > PS10 > PS6. PS6 and PS10 were selected as preselected membranes for the influencing factors of the later research considering the deviation of practical application. The Cd^{2+} concentration after ultrafiltration with different pore size membranes was significantly different at 120 min (Fig. 6). The amount of concentration of Cd^{2+} showed the following tendency: PVDF > PS50 > PS10 > PS6. The concentration of Cd^{2+} in the ultrafiltration membrane permeation liquid with PS6 reached the first level emission standard of GB 8978-1996 (<0.1 mg/L), and PS6 was selected as the preselected membrane for the influencing factors in the later research.

3.2. Permeate flux

The initial membrane fluxes of PS6, PS10, PS50, and PVDF were 12.59, 15.80, 36.25 and 42.50 $L/m^2 \cdot h$, respectively. The permeate flux of Cu^{2+} was significantly affected by

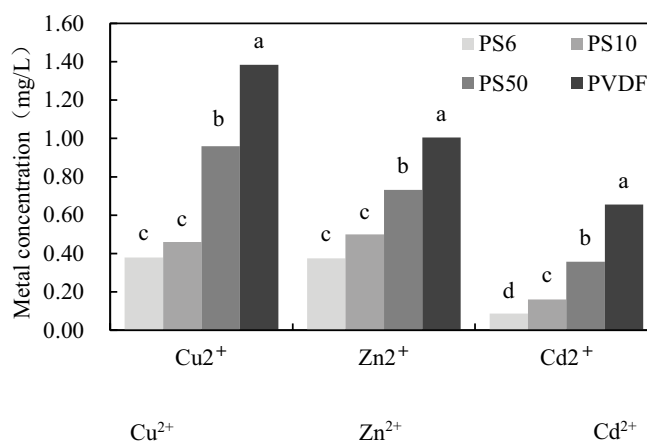


Fig. 6. The concentration of heavy metals after ultrafiltration treatment by four pore membranes for heavy metal wastewater complexed by palygorskite.

membrane pore diameter (Table 1). The permeate fluxes of four kinds of the membrane at different times (30 min intervals) were significantly different. There was a very significant difference in permeate flux between the four membrane pore sizes at 30 min, where the membrane fluxes of the four membrane pore sizes were 11.67, 14.73, 28.07, and 38.56 $L/m^2 \cdot h$, respectively, and PS50 had the smallest permeate flux. Membrane pore diameter was not significantly different among PS6, PS10, and PVDF, and was significantly higher than it in PS50. The membrane fluxes of the four membrane pore sizes were 10.60, 13.50, 22.23, 28.58 $L/m^2 \cdot h$, respectively when the time was 60 min. There was no significant difference in the permeate flux between PS6 and PS10. The fluxes of the four membrane pores were 9.07, 10.93, 16.44 and 15.60 $L/m^2 \cdot h$, respectively, and the permeate flux of PVDF was the smallest when the time was 90 min. The membrane pore diameter was not significantly different between PS6 and PS10, and was significantly higher than others. The membrane fluxes of the four membrane pore sizes were 7.37, 8.44, 12.64 and 10.10 $L/m^2 \cdot h$, respectively when the time were 120 min. There was no significant difference in the permeate flux between PS6 and PS10. The membrane fluxes of the four membrane pore sizes were 6.96, 7.72, 10.53 and 8.38 $L/m^2 \cdot h$, respectively, and the permeate flux of PS6 was significantly larger than PS10 when the time was 150 min. The flux of PS10 was always greater than PS6 and there was no significant difference between the PS6 and PS10 during the whole operating period of heavy metal Cu^{2+} . PS10 was chosen as the influential factors for the heavy metal Cu^{2+} in the latter study (Table 1).

The permeate fluxes of Zn^{2+} were affected by the four membrane pore sizes. The permeate fluxes of four kinds of the membrane at different times (30 min intervals) were significantly different. The membrane fluxes of the four membrane pore sizes were 12.38, 14.13, 31.95 and 37.48 $L/m^2 \cdot h$, respectively, and the permeate flux of PS6 was the largest when the running time was 30 min. Membrane pore diameter was not significantly different among PS10, PS50, and PVDF. The membrane fluxes of the four membrane pore sizes were 11.00, 11.90, 20.86 and 26.00 $L/m^2 \cdot h$, respectively, and

Table 1
Influence of membrane pore size on normalization membrane specific flux in the process of complexation–ultrafiltration of heavy metals by palygorskite

Metal	MWCO	30 min	60 min	90 min	120 min	150 min
Cu ²⁺	PS6	0.93 ± 0.02a	0.84 ± 0.02a	0.72 ± 0.014a	0.58 ± 0.01a	0.55 ± 0.01a
	PS10	0.93 ± 0.06a	0.85 ± 0.05a	0.69 ± 0.041a	0.53 ± 0.03a	0.49 ± 0.03b
	PS50	0.77 ± 0.01b	0.61 ± 0.01b	0.45 ± 0.005b	0.35 ± 0.01b	0.29 ± 0.01c
	PVDF	0.91 ± 0.04a	0.67 ± 0.03b	0.37 ± 0.018c	0.24 ± 0.01c	0.20 ± 0.01d
	F-value	12.02**	43.14***	160.19***	238.23***	305.62***
Zn ²⁺	PS6	0.96 ± 0.02a	0.86 ± 0.02a	0.76 ± 0.01a	0.61 ± 0.01a	0.52 ± 0.01a
	PS10	0.91 ± 0.02b	0.76 ± 0.01b	0.61 ± 0.01b	0.51 ± 0.01b	0.47 ± 0.01b
	PS50	0.87 ± 0.02b	0.57 ± 0.01d	0.36 ± 0.01d	0.28 ± 0.01c	0.24 ± 0.01c
	PVDF	0.88 ± 0.02b	0.61 ± 0.01c	0.40 ± 0.01c	0.21 ± 0.01d	0.17 ± 0.01d
	F-value	15.44**	325.89***	13,743.24***	1,419.81***	1,241.91***
Cd ²⁺	PS6	0.93 ± 0.02b	0.86 ± 0.02b	0.82 ± 0.01a	0.71 ± 0.01a	0.66 ± 0.01a
	PS10	0.96 ± 0.01a	0.90 ± 0.01a	0.80 ± 0.02a	0.69 ± 0.04a	0.63 ± 0.01b
	PS50	0.86 ± 0.01c	0.80 ± 0.01c	0.74 ± 0.02b	0.63 ± 0.04b	0.42 ± 0.01c
	PVDF	0.93 ± 0.01b	0.72 ± 0.01d	0.59 ± 0.02c	0.46 ± 0.03c	0.37 ± 0.01d
	F-value	33.21***	208.30***	89.59***	37.48***	514.21***

The same letter number indicates that there is no significant difference among four pore membranes; ****P* < 0.001; **0.001 < *P* < 0.01; *0.01 < *P* < 0.05.

there was a significant difference in the permeate flux among the four membranes when the running time was 60 min. The fluxes of the four membrane pores were 9.80, 9.54, 13.16 and 17.00 L/m²·h, respectively, and there was a significant difference in the permeate flux among the four membranes when the running time was 90 min. The membrane fluxes of the four membrane pore sizes were 7.87, 7.91, 10.05 and 9.10 L/m²·h, respectively, and there was a significant difference in the permeate flux among the four membranes at 120 min. The membrane fluxes of the four membrane pore sizes were 6.61, 7.37, 8.73 and 7.29 L/m²·h, respectively, and there was a significant difference in the permeate flux among the four membranes at 150 min. The normalized membrane specific fluxes were listed in order from high to low as PS6, PS10, PS50, and PVDF. The normalized membrane specific flux of PS6 was significantly greater than PS10 during the entire process. However, the permeate flux of PS10 was greater than PS6. It was concluded that PS10 was suitable for the treatment of Zn²⁺ (Table 1).

The permeate fluxes of Cd²⁺ were affected by the four membrane pore sizes. For the five times from four membrane pore sizes a significant difference was found. The membrane fluxes of the four membrane pore sizes were 11.75, 15.29, 31.56 and 39.48 L/m²·h, respectively, and the permeate flux of PS10 was the largest when the time was 30 min. There were significant differences in the permeate fluxes among PS6, PS10, and PS50. The membrane fluxes of the four membrane pore sizes were 10.80, 14.26, 29.28 and 30.64 L/m²·h, respectively, and there was a significant difference in the permeate flux among the four membranes at 60 min. The fluxes of the four membrane pores were 10.29, 12.66, 26.97 and 25.11 L/m²·h, respectively when the running time was 90 min. There was no significant difference in permeate flux between PS6 and PS10. The fluxes of the four membrane pores were 8.97, 10.98, 22.84, and 19.63 L/

m²·h, respectively when the running time was 120 min. There was no significant difference in permeate flux between PS6 and PS10. The fluxes of the four membrane pores were 8.27, 10.07, 15.48, and 15.66 L/m²·h, respectively, and there was a significant difference in the permeate flux among the four membranes at 150 min. The order of the normalized membrane specific fluxes for the four membranes was PS6 > PS10 > PS50 > PVDF. The permeate flux of PS6 was significantly larger than PS10 in the experiment. PS6 was selected as the pore size of the influential factors for the later research of heavy metal Cd²⁺ (Table 1).

3.3. Effect of time on membrane fouling

The evolution of permeate flux with time for all the membranes was tested at a transmembrane pressure of 1 bar, and a temperature of 20°C. The permeate fluxes of PS50 and PVDF showed a sharp decrease in 0 to 100 min (Fig. 7). But it was not observed for the membranes of PS6 and PS10, which showed a much lower flux decline rate. This can be attributed to the fact that the PS50 and PVDF showed an MWCO much closer to the size of raw water particles than PS6 and PS10. Permeate flux achieved steady-state values after about 140 min of operation for all the membranes tested. Among all the membranes tested, the PS6 showed the lowest flux decline (44.72%) during the fouling step in comparison with the PS10 (51.14%), the PVDF (80.28%), and the PS50 (70.96%).

The evolution of permeate flux with time for all the membranes tested at a transmembrane pressure of 1 bar, a temperature of 20°C. When ultrafiltration membrane is used to remove Zn²⁺ (Fig. 8). Permeate flux achieved steady-state values after about 130 min of operation for all the membranes tested. The experimental data that corresponds to the membrane of PS50 and PVDF show a sharp flux in

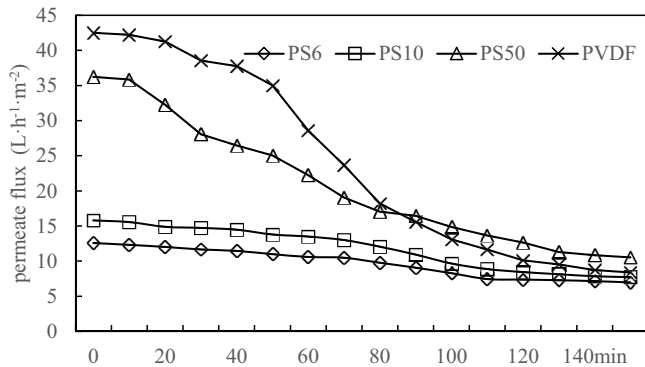


Fig. 7. Evolution of permeate flux with time for ultrafiltration treatment of wastewater contained Cu^{2+} complexed by palygorskite

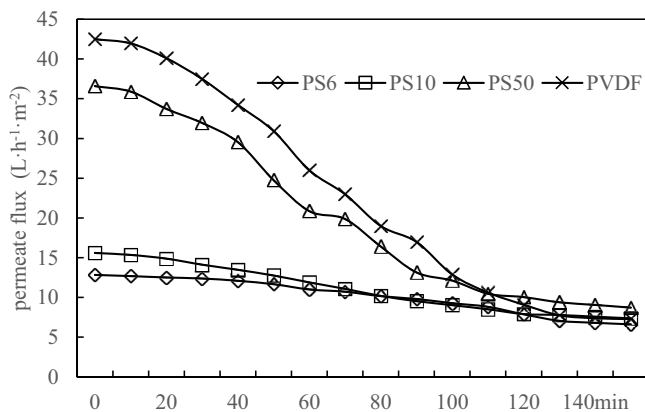


Fig. 8. Evolution of permeate flux with time for ultrafiltration treatment of wastewater contained Zn^{2+} complexed by palygorskite.

0–130 min. This is not observed for the membranes of PS6 and PS10, which show a sharp flux in 70–110 min decline rate. Among all the membranes tested, the PS50 showed the fastest flux decline (82.84%) during the fouling step in comparison with the PS10 (52.79%), the PS6 (48.52%), and the PS50 (76.13%).

The evolution of permeate flux with time for all the membranes tested at a transmembrane pressure of 1 bar, a temperature of 20°C , When ultrafiltration membrane is used to remove Cd^{2+} (Fig. 9). Permeate flux declined gradually and finally stabilized after about 140 min of operation for all the membranes tested. The experimental data that corresponds to the membrane of PVDF show a sharp flux. The permeate flux decreased gradually with the time, which significantly declined when the time is 30–70 min. This is not observed for the membranes of PS6, PS10 and PS50, which show a much lower flux decline rate.

When an ultrafiltration membrane was used to filter palygorskite, the evolution of permeate flux with time is shown in Fig. 10. Permeate flux with time declined accordingly for PS50 and PVDF. The membranes of PS6 and PS10, showed a much lower flux decline rate. This can be attributed to the fact that the PS50 and PVDF show

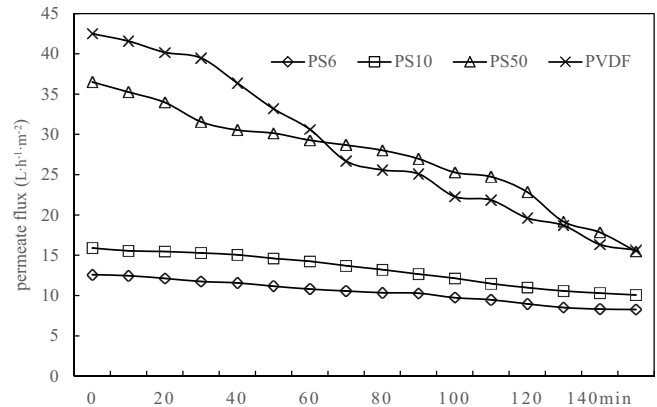


Fig. 9. Evolution of permeate flux with time for ultrafiltration treatment of wastewater contained Cd^{2+} complexed by palygorskite.

much closer to the size of raw water particles than PS6 and PS10.

3.4. Influence of heavy metals on membrane specific flux

The experimental data that corresponds to the membrane of PS6, PS10, PS50, and PVDF show the evolution of the value of J_s/J_0 (Fig. 11). When PS6, PS10, PS50, and PVDF were used to remove Zn^{2+} and Cu^{2+} , the value of J_s/J_0 had a significant difference, but the normalized membrane specific flux of PVDF was significantly lower than the normalized membrane specific flux of PS6, PS10, and PS50, and normalized membrane specific flux of PS6 was significantly higher than that of other treatments. When ultrafiltration membrane was used to remove Cd^{2+} , normalized membrane specific flux of PS6 and PS10 had no significant difference, but normalized membrane specific flux of PS6 and PS10 was significantly higher than normalized membrane specific flux of PS50 and PVDF.

3.5. Evolution of resistance for four ultrafiltration membrane

Among all the membranes tested, when dealing with heavy metal Cd^{2+} , the percentage of R_m are the highest in all the films during the fouling step in comparison with other heavy metal (Fig. 12). For PS6 and PS10, the ratio of the resistance of the membrane to the total resistance is the highest. This is not observed for the membranes of PS50 and PVDF, the highest proportion of its resistance distribution is the filter cake layer resistance. This can be attributed to the fact that the types of materials affect the distribution of resistance. When dealing with heavy metal Zn^{2+} and Cu^{2+} , the concentration polarization resistance of PVDF is the highest in all the membranes during the fouling step in comparison with membranes. For all heavy metals, the blockage resistance of the membrane is the lowest in all the membranes during the fouling step in comparison with R_m , R_{cp} , and R_c . For the filter cake layer resistance in PS6 and PS10 had a significant difference with the change of heavy metals. This can be attributed to the fact that the concentration of heavy metals affects the contamination of the filter cake layer.

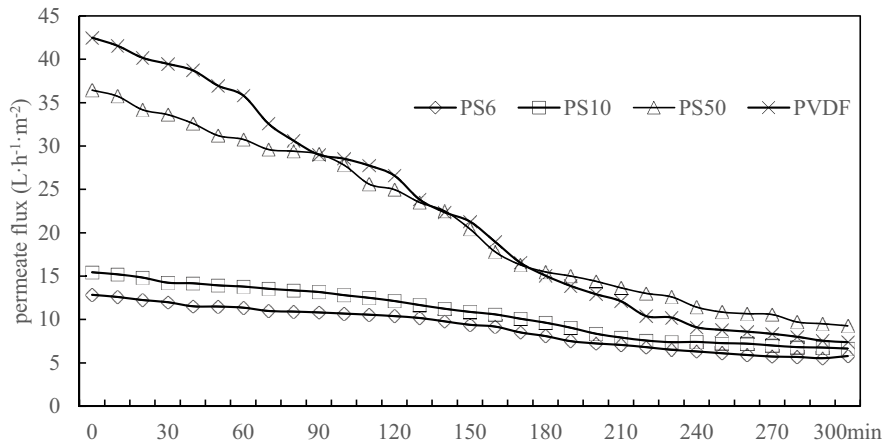


Fig. 10. Evolution of permeate flux with time when ultrafiltration membranes are used to filter palygorskite.

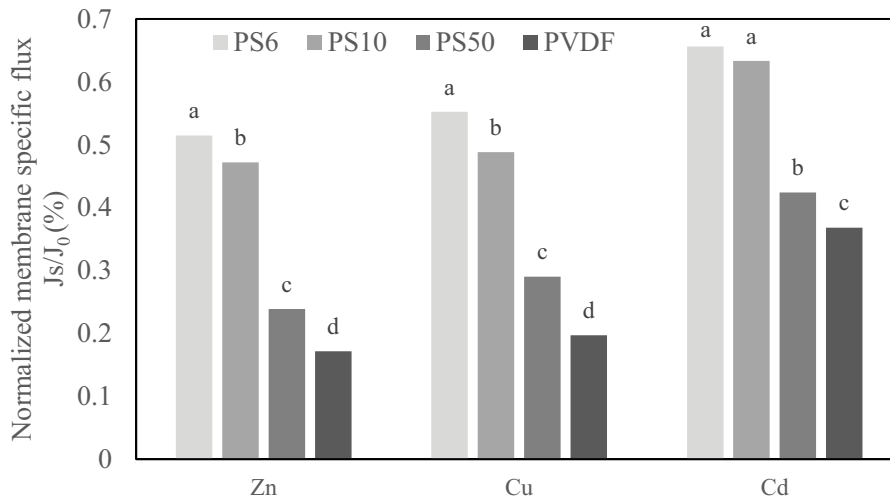


Fig. 11. Influence of four kinds of ultrafiltration membrane specific flux for four kinds of ultrafiltration treatment of wastewater contained Zn, Cu and Cd complexed by palygorskite.

4. Conclusions and discussions

The concentration of palygorskite was 5 g/L, and the concentration of copper, zinc, and cadmium was 40, 30, and 10 mg/L under the condition of pH = 7. Palygorskite complex heavy metal ion ultrafiltration membrane was retained by the hollow fiber ultrafiltration membrane of 6,000; 10,000; 50,000 and 100,000 Da, respectively, and the heavy metal Cu²⁺, Zn²⁺, and Cd²⁺ were kept stable in 120, 90, 120 min, respectively. The effect was to intercept the Cu²⁺ and Zn²⁺ concentration of the ultrafiltration membrane permeation water with a molecular weight of 6,000 and 10,000 Da, and the Cd²⁺ concentration of the effluent from the ultrafiltration membrane-permeable liquid with the molecular weight of 6,000 Da could reach the first-grade discharge standard of the comprehensive sewage discharge standard of GB 8978-1996. The heavy metal ions can be effectively intercepted by the ultrafiltration membrane after the adsorption. The removal rate of this experiment is much higher than that of palygorskite complex experiment

or single membrane ultrafiltration experiment. It may be the effect of ultrafiltration membrane interception and the effect of palygorskite fully rod crystal dissociation.

The normalized difference of the 6,000 and 10,000 Da was smaller than that of the flux, the decrease of the normalized membrane flux was smaller, the normalized flux of 50,000 and 100,000 Da was greatly reduced, and the flux of the normalized membrane decreased sharply during the ultrafiltration process of heavy metals Cu²⁺, Zn²⁺, and Cd²⁺. The 10,000 Da ultrafiltration membrane was selected as the suitable ultrafiltration membrane pore size for Cu²⁺ and Zn²⁺, and the 6,000 Da ultrafiltration membrane was suitable for the ultrafiltration membrane pore size of Cd²⁺. The adsorption of palygorskite on heavy metals in wastewater made the surface of the membrane formed deposition layer, the surface of the membrane was smaller than the cake resistance. The probability of the particles entering the small aperture was much smaller than that of the large aperture. The membrane flux reduced as the membrane pore plugging pollution increased.

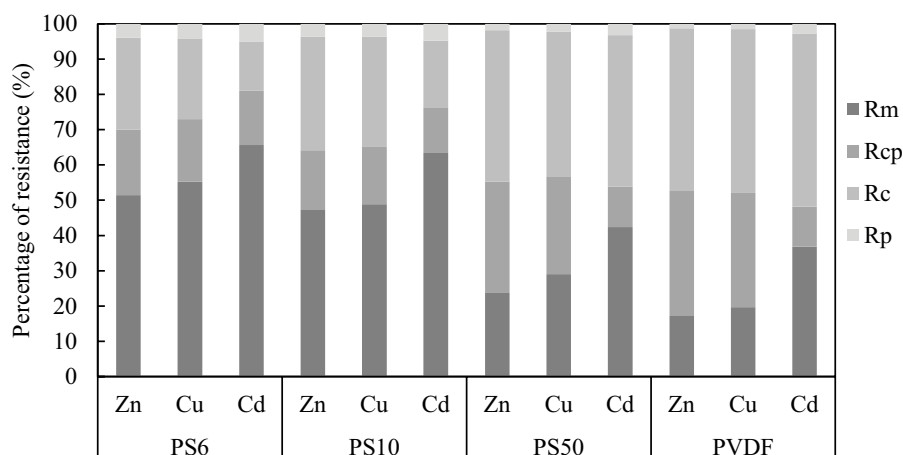


Fig. 12. Evolution of resistance for four kinds of ultrafiltration membrane treatment of wastewater contained Zn^{2+} , Cu^{2+} and Cd^{2+} complexed by palygorskite.

The rejection coefficient and permeate flux of palygorskite decreased due to the fact that the organic complexing agent had almost no rejection coefficient for Cu^{2+} , Zn^{2+} , and Cd^{2+} . However, considering the simple fabrication and easy handle of palygorskite, it is very promising to be used as a high-performance complexing agent for heavy metal removal.

Along with the increase of time, the permeation flux decreased. Permeate flux declined gradually and finally stabilized after about 140 min of operation for all the membranes tested. The PVDF showed the highest flux decline, during the fouling step in comparison with the PS6, PS10, PS50, and PVDF. The flux decline for PVDF when dealing with heavy metals Zn^{2+} , Cu^{2+} , and Cd^{2+} are 82.84%, 80.28%, and 63.16%. When an ultrafiltration membrane is used to remove Zn^{2+} and Cu^{2+} , J_s/J_0 of PS6, PS10, PS50, and PVDF had a significant difference. When ultrafiltration membrane is used to remove Cd, J_s/J_0 of PS6 and PS10 had no significant difference, but J_s/J_0 of PS6 and PVDF was significantly higher than J_s/J_0 of PS50 and PVDF. The concentration of heavy metals and types of materials affect the distribution of resistance. For PS6 and PS10, the ratio of the resistance of the membrane to the total resistance is the highest. This is not observed for the membranes of PS50 and PVDF, the highest proportion of its resistance distribution is the filter cake layer resistance. The filter cake layer resistance in PS6 and PS10 had a significant difference with the change of heavy metals.

Acknowledgements

This research was supported by the Open Foundation of Key Laboratory of Yellow River Environment of Gansu Province, (20JR2RA002, 21YRWEK007, 21YRWEG003); Industrial Support Program of Education Department of Gansu Province, (2021CYZC-31); Innovation and Entrepreneurship Talent Project of Lanzhou, (2021-RC-41).

References

- [1] N.H. Baharuddin, N.M.N. Sulaiman, M.K. Aroua, Removal of zinc and lead ions by polymer-enhanced ultrafiltration using

unmodified starch as novel binding polymer, *Int. J. Environ. Sci. Technol.*, 12 (2015) 1825–1834.

- [2] K.R. Desai, Z.V.P. Murthy, Removal of Ag(I) and Cr(VI) by complexation-ultrafiltration and characterization of the membrane by CFSK model, *Sep. Sci. Technol.*, 49 (2014) 2620–2629.
- [3] S. Malamis, E. Katsou, T. Kosanovic, K.J. Haralambous, Combined adsorption and ultrafiltration processes employed for the removal of pollutants from metal plating wastewater, *Sep. Sci. Technol.*, 47 (2012) 983–996.
- [4] Ghadge, Chavan, Divekar, Vibhandik, Pawar, Marathe, Mathematical modelling for removal of mixture of heavy metal ions from waste-water using micellar enhanced ultrafiltration (MEUF) process, *Sep. Sci. Technol.*, 50 (2015) 365–372.
- [5] V.C. Fenelon, J.H. Miyoshi, C.S. Mangolim, A.S. Noce, L.N. Koga, G. Matioli, Different strategies for cyclodextrin production: ultrafiltration systems, CGTase immobilization and use of a complexing agent, *Carbohydr. Polym.*, 192 (2018) 19–27.
- [6] M.A. Khosa, S.S. Shah, X. Feng, Thermodynamic functions of metal-sericin complexation in ultrafiltration study, *J. Membr. Sci.*, 470 (2014) 1–8.
- [7] S. Zhou, A. Xue, Y. Zhang, M. Li, K. Li, Y. Zhao, W. Xing, Novel polyamidoamine dendrimer-functionalized palygorskite adsorbents with high adsorption capacity for Pb^{2+} and reactive dyes, *Appl. Clay Sci.*, 107 (2015) 220–229.
- [8] R.W. Field, G.K. Pearce, Critical, sustainable and threshold fluxes for membrane filtration with water industry applications, *Adv. Colloid Interface Sci.*, 164 (2011) 38–44.
- [9] S. Li, S.G.J. Heijman, J.Q.J.C. Verberk, G.L. Amy, J.C. van Dijk, Seawater ultrafiltration fouling control: backwashing with demineralized water/SWRO permeate, *Sep. Purif. Technol.*, 98 (2012) 327–336.
- [10] T. Lin, Z.J. Lu, W. Chen, Interaction mechanisms of humic acid combined with calcium ions on membrane fouling at different conditions in an ultrafiltration system, *Desalination*, 357 (2015) 26–35.
- [11] A. Resosudarmo, Y. Ye, P. Le-Clech, V. Chen, Analysis of UF membrane fouling mechanisms caused by organic interactions in seawater, *Water Res.*, 47 (2013) 911–921.
- [12] C. Wang, Q. Li, H. Tang, D. Yan, W. Zhou, J. Xing, Y. Wan, Membrane fouling mechanism in ultrafiltration of succinic acid fermentation broth, *Bioresour. Technol.*, 116 (2012) 366–371.
- [13] H. Chang, F. Qu, B. Liu, H. Yu, K. Li, Hydraulic irreversibility of ultrafiltration membrane fouling by humic acid: effects of membrane properties and backwash water composition, *J. Membr. Sci.*, 493 (2015) 723–733.
- [14] H. Yamamura, K. Okimoto, K. Kimura, Y. Watanabe, Hydrophilic fraction of natural organic matter causing irreversible fouling

- of microfiltration and ultrafiltration membranes, *Water Res.*, 54 (2014) 123–136.
- [15] Y. He, J. Sharma, R. Bogati, B.Q. Liao, C. Goodwin. Impacts of aging and chemical cleaning on the properties and performance of ultrafiltration membranes in potable water treatment, *Sep. Sci. Technol.*, 49 (2014) 1317–1325.
- [16] L. Ma, S. Wang, S. Li, G.J. Heijman, L.C. Rietveld, X.B. Su, Practical experience of backwashing with RO permeate for UF fouling control treating surface water at low temperatures, *Sep. Purif. Technol.*, 119 (2013) 136–142.
- [17] F. Xiao, P. Xiao, W.J. Zhang, D.S. Wang, Identification of key factors affecting the organic fouling on low-pressure ultrafiltration membranes, *J. Membr. Sci.*, 447 (2013) 144–152.
- [18] J.X. Zeng, H.Q. Ye, N.D. Huang, J.F. Liu, L.F. Zheng, Selective separation of Hg(II) and Cd(II) from aqueous solutions by complexation-ultrafiltration process, *Chemosphere*, 76 (2009) 706–710.
- [19] Y. Qiu, L. Mao, W. Wang, Removal of manganese from waste water by complexation-ultrafiltration using copolymer of maleic acid and acrylic acid, *Trans. Nonferrous Met. Soc. China*, 24 (2014) 1196–1201.
- [20] S. Jana, A. Saikia, M.K. Purkait, K. Mohanty, Chitosan based ceramic ultrafiltration membrane: preparation, characterization and application to remove Hg(II) and As(III) using polymer enhanced ultrafiltration, *Chem. Eng. J.*, 170 (2011) 209–219.
- [21] Y. Feng, Y. Wang, Y. Wang, S. Liu, J. Jiang, C. Cao, J. Yao, Simple fabrication of easy handling millimeter-sized porous palygorskite/polymer beads for heavy metal removal, *J. Colloid Interface Sci.*, 502 (2017) 52–58.
- [22] Y. Liu, J. Xu, W. Wang, A. Wang, Effects of sodium salts organic acids modification on the microstructure and dispersion behavior of palygorskite nano-powder via high-pressure homogenization process, *J. Dispersion Sci. Technol.*, 35 (2014) 840–847.
- [23] W. Wang, A. Wang, Nanocomposite of carboxymethyl cellulose and palygorskite as a novel pH-sensitive superabsorbent: synthesis, characterization and properties, *Carbohydr. Polym.*, 82 (2010) 83–91.
- [24] B. Lam, S. Déon, N. Morin-Crini, G. Crini, P. Fievet, Polymer-enhanced ultrafiltration for heavy metal removal: influence of chitosan and carboxymethyl cellulose on filtration performances, *J. Cleaner Prod.*, 171 (2018) 927–933.
- [25] L. Ni, P. Zhang, J. Chen, J. Jiang, S. Ding, Iso-propanol assisted preparation of individualized functional palygorskite fibers and its impact on improving dispersion abilities in polymer nanocomposites, *Korean J. Chem. Eng.*, 34 (2017) 1827–1833.
- [26] A.Z. El-Sonbati, M.A. Diab, A.A. El-Bindary, A.M. Eldesoky, S.M. Morgan, Correlation between ionic radii of metals and thermal decomposition of supramolecular structure of azodye complexes, *Spectrochim. Acta, Part A*, 135 (2015) 774–791.
- [27] E. Abbasi-Garravand, C.N. Mulligan, Using micellar enhanced ultrafiltration and reduction techniques for removal of Cr(VI) and Cr(III) from water, *Sep. Purif. Technol.*, 132 (2014) 505–512.
- [28] P.S. Goh, B.C. Ng, W.J. Lau, A.F. Ismail, Inorganic nanomaterials in polymeric ultrafiltration membranes for water treatment, *Sep. Purif. Rev.*, 44 (2015) 216–249.
- [29] J.H. Huang, G.M. Zeng, C.F. Zhou, X. Li, L.J. Shi, S.B. He, Adsorption of surfactant micelles and Cd²⁺/Zn²⁺ in micellar-enhanced ultrafiltration, *J. Hazard. Mater.*, 183 (2010) 287–293.
- [30] F. Qu, H. Liang, J. Zhou, J. Nan, S. Shao, J. Zhang, G. Li, Ultrafiltration membrane fouling caused by extracellular organic matter (EOM) from *Microcystis aeruginosa*: effects of membrane pore size and surface hydrophobicity, *J. Membr. Sci.*, 449 (2014) 58–66.
- [31] M.J. Corbatón-Báguena, S. Álvarez-Blanco, M.C. Vincent-Vela, J. Lora-García, Utilization of NaCl solutions to clean ultrafiltration membranes fouled by whey protein concentrates, *Sep. Purif. Technol.*, 150 (2015) 95–101.
- [32] R.H. Peiris, M. Jaklewicz, H. Budman, R.L. Legge, C. Moresoli, Assessing the role of feed water constituents in irreversible membrane fouling of pilot-scale ultrafiltration drinking water treatment systems, *Water Res.*, 47 (2013) 3364–3374.
- [33] H.Y. Fan, M. Nazari, G. Raval, Z. Khan, H. Patel, Utilizing zeta potential measurements to study the effective charge, membrane partitioning, and membrane permeation of the lipopeptide surfactin, *Bba-biomembranes*, 1838 (2014) 2306–2312.
- [34] J.H. Jhaveri, Z.V.P. Murthy, A comprehensive review on anti-fouling nanocomposite membranes for pressure driven membrane separation processes, *Desalination*, 379 (2016) 137–154.
- [35] X. Shi, G. Tal, N.P. Hankins, V. Gitisb, Fouling and cleaning of ultrafiltration membranes: a review, *J. Water Process Eng.*, 1 (2014) 121–138.
- [36] D.G. Kim, H. Kang, S. Han, J.C. Lee, Dual effective organic/inorganic hybrid star-shaped polymer coatings on ultrafiltration membrane for bio- and oil-fouling resistance, *ACS Appl. Mater. Interfaces*, 4 (2016) 5898–5906.
- [37] S. Shao, H. Liang, F. Qu, H.R. Yu, K. Li, G.B. Li, Fluorescent natural organic matter fractions responsible for ultrafiltration membrane fouling: identification by adsorption pretreatment coupled with parallel factor analysis of excitation-emission matrices, *J. Membr. Sci.*, 464 (2014) 33–42.
- [38] J. Shao, J. Hou, H.C. Song, Comparison of humic acid rejection and flux decline during filtration with negatively charged and uncharged ultrafiltration membranes, *Water Res.*, 45 (2011) 473–482.
- [39] M.G. Nainar, K. Jayaraman, H.K. Meyyappan, L.R. Miranda, Antifouling properties of poly(vinylidene fluoride)-incorporated cellulose acetate composite ultrafiltration membranes, *Korean J. Chem. Eng.*, 37 (2020) 2248–2261.
- [40] M. Wang, Z. Li, J. Li, F. Yan, T. Zhang, F. Qin, J. Zhang, Preparation of chitosan graft benzo-15-crown-5/non-woven fabric composite membrane for enhanced Pd; adsorptive separation, *Sep. Sci. Technol.*, 56 (2021) 1140–1151.
- [41] J. Huang, L. Peng, G. Zeng, X. Li, Y. Zhao, L. Liu, F. Li, Q. Chai, Evaluation of micellar enhanced ultrafiltration for removing methylene blue and cadmium ion simultaneously with mixed surfactants, *Sep. Purif. Technol.*, 125 (2014) 83–89.
- [42] Y. Huang, D. Wu, X. Wang, W. Huang, D. Lawless, X. Feng, Removal of heavy metals from water using polyvinylamine by polymer-enhanced ultrafiltration and flocculation, *Sep. Purif. Technol.*, 158 (2016) 124–136.
- [43] S. Tang, Y. Qiu, Removal of Zn(II) by complexation-ultrafiltration using rotating disk membrane and the shear stability of PAA-Zn complex, *Korean J. Chem. Eng.*, 35 (2018) 2078–2085.